FT-IR, FT-Raman, Molecular Geometry, Vibrational Assignments, Ab-Initio and Density Functional Theory Calculations for 4-hydroxy-2,6-dimethyl pyrimidine

A. Janaki[1], V. Balachandran[2], A. Lakshmi[3]

[1]Department of Physics, Govt. Arts College for Women (Autonomous), Pudukkottai 622 001, India

[2]Department of Physics, Arignar Anna Govt. Arts College, Musiri 621 201, India

[3]Department of Physics, Govt. Arts College, Tiruchirappalli 620 022, India

Abstract: *Fourier transform Raman and infrared spectra of 4-hydroxy-2,6-dimethyl pyrimidine (HDMP) were recorded and interpreted by comparison with respective theoretical spectra calculated using HF and B3LYP methods. The HDMP equilibrium geometry with C_s symmetry, harmonic vibrational frequencies, infrared and Raman intensities were determined using HF/6-311G and B3LYP/6-311G level of theories. The band assignment was based on potential energy distribution (PED) of normal modes. A sufficient general agreement between the theoretical and experimental spectra has been achieved. In the computed equilibrium geometries by all the levels, the bond lengths and bond angles show changes in the neighborhood of methyl and hydroxyl substituent. The molecular stability and bond strength were investigated by applying the Natural Bond Orbital analysis (NBO). The calculated HOMO-LUMO energies shows that charge transfer occur in the molecule. The dipole moment, polarizability and the hyperpolarizability values of the investigated molecule have been computed using HF and B3LYP methods.*

Keywords: 4-hydroxy-2,6-dimethyl pyrimidine ; Vibrational spectra; NBO; HOMO– LUMO; Hyperpolarizability

1. Introduction

Pyrimidine and its derivatives are known for their biological and pharmaceutical importance. Their properties are determined by hydrogen and π-bonding systems. They are belonging to the family of nucleic acids. Nucleic acids are of great interest, since they control the manufacture of protein and functions of the cells in living organism. Due to the significant role of N-heterocyclic molecules (i.e., cytosine, Uralic and thymine etc.) in the structural problems of nucleic acid, investigations on the substituted pyrimidines draw considerable attention [1–3].

Literature survey reveals that to the best of our knowledge, the results based on quantum chemical calculations, FT-IR and FT-Raman spectral studies and NBO analysis on 4-hydroxy-2,6-dimethyl pyrimidine (HDMP) have not been reported. This inadequacy observed in the literature encouraged us to make this theoretical and experimental vibrational spectroscopic research based on the structure of molecules to give a correct assignment of the fundamental bands in experimental FT-IR, FT-Raman spectra.

The first purpose of this work is to investigate the performance of different DFT methods in predicting geometry and vibrational spectra of HDMP. The second purpose of this work is to study the thermodynamic functions and bonding nature of HDMP by using HF and B3LYP level of theories throughout with the 6-311G basis set implemented in the Gaussian 09 program suite [4]. The calculations of potential energy distribution (PED) were done on a PC with the version V7.0-G77 of the MOLVIB program written by Sundius [5, 6].

The third purpose of this work is to study the natural bond orbital analysis (NBO), electrostatic potential should help us to understand the structural and spectral characteristic and bioactivity of compounds of this class. Optimized geometry obtained from DFT calculation was then used to perform NBO analysis. This study provided a wealth of theoretical data giving insights into the kinetic and structural behavior of HDMP. A fundamental understanding of the properties of HDMP is believed to be essential for the development of the drug designing.

2. Experimental Details

The compound HDMP was purchased from Lancaster Chemical Company, UK, with a stated purity of 99% and it was used as such without further purification. The FT-Raman spectrum of HDMP was recorded using 1064 nm line of Nd:YAG laser as excitation wave length in the region 3500−100 cm^{-1} on thermo electron corporation model BRUKER IFS 66 vacuum fourier transform spectrophotometer equipped with FT-Raman module accessory. The FT-IR spectrum of the title compound was recorded in the region 4000−400 cm^{-1} on with same instrument in KBr pellet technique. The spectrum was recorded at room temperature with a scanning speed of 30 cm^{-1} min^{-1} and the spectral width of 2.0 cm^{-1}. The observed experimental FT-IR and FT-Raman spectra and theoretically predicted IR and Raman spectra at HF/6-311G and

B3LYP/6-311G levels are shown in Figs. 1 and 2, respectively.

3. Computational Details

Quantum chemical calculations were used for HDMP to carry out the optimized geometry and vibrational wavenumbers with the 2009 version of the Gaussian suite program [4] using the HF and B3LYP functional [7, 8] supplemented with standard 6-311G basis set. For the plots of simulated IR and Raman spectra, pure Lorentzian band shapes were used with a band width (FWHM) of $\pm$ 10 cm^{-1}. The vibrational modes were assigned by means of visual inspection using the GAUSSVIEW Program [9]. The analysis for the vibrational modes of HDMP is presented in some detail in order to better describe the basis for the assignments. From the basic theory of Raman scattering, Raman activities (s_i) calculated by Gaussian 09W Program has been converted to relative Raman intensities (I_i) using the following relationship [10, 11]:

$$I_i = \frac{f(\upsilon_0 - \upsilon_i)^4 s_i}{\upsilon_i [1 - \exp(-hc\upsilon_i)]/kT} \qquad \dots (1)$$

where υ_0 is the exciting wavenumber (in cm^{-1}), υ_i is the vibrational wavenumber of the ith normal mode, $h, c,$ and k are universal constant and f is a suitably chosen common normalization factor for all the peak intensities.

Natural bond orbital analysis was also performed by the Gaussian 09W Program at the B3LYP level of theory analysis transforms the canonical delocalized Hartee-Fock (HF) molecular orbital (MO) into localized MOs that are closely tied to chemical bonding concepts. This process involves sequential transformation of non-orthogonal atomic orbital's (*AOs*) to the sets of natural atomic orbital's (*NAOs*), natural hybrid orbital's (*NHOs*) and natural bond orbital. The localized basis sets are completely describes the wave functions in the most economic method, as electron density and other properties that are described by the minimal amount of filled NBOs describe the hypothetical, strictly localized Lewis structure. The interaction between filled and anti-bonding (or Rydberg) orbital represent the deviation of the molecule from the Lewis structure and can be used as the measure of delocalization. This non-covalent bonding anti-bonding charge transfer interactions can be quantitatively described in terms of the second-order perturbation interaction energy ($E^{(2)}$) [11-15]. This energy represents the estimate of the off-diagonal NBO Fock matrix elements. It can be deduced from the second-order perturbation approach [16] as follows:

$$E^{(2)} = \Delta E_{ij} = q_i \frac{F_{(i,j)}^2}{\varepsilon_j - \varepsilon_i} \qquad \dots (2)$$

where q_i is the ith donor orbital occupancy, $\varepsilon_j, \varepsilon_i$ the diagonal elements (orbital energies) and $F_{(j,i)}$ the off diagonal NBO Fock matrix element.

4. Results and Discussion

4.1 Geometrical Structure

The optimized structural parameters and global minimum energy of HDMP were calculated by C_s point group symmetry with HF/6-311G and B3LYP/6-311G levels. In accordance with the atom numbering scheme the optimized geometrical structure is given in Fig. 3.

The global minimum energy of HDMP in C_s point group symmetry with HF and B3LYP methods are collected in Table 1. The C_2 conformer has minimum energy value as compared to C_1 conformer. The optimized structure can be compared with other similar system for which the crystal structures have been solved already. Therefore, the optimized geometrical parameters of pyrimidine [17] are compared to those of title compound. The comparative optimized structural parameters were presented in Table 2.

From the theoretical values we can find that most of the optimized bond lengths and bond angles are slightly longer and shorter than the experimental values. These variations are due to the nature and position of the substituents. By comparing HF and B3LYP methods, B3LYP values are much closer to experimental values due to the inclusion of electron correlation.

4.2 Effect of multiple scaling on frequency fit and vibrational assignments

The vibrational frequencies obtained by density functional theory calculations are known for over estimation from the experimental values by 2–7% on average. A tentative assignment is often made on the basis of unscaled computed frequency by assuming the observed frequency so that they are in the same order as the calculated ones. Then, for an easier comparison to the observed values, the calculated frequencies are scaled by the scale factors of less than 1, to minimize the overall deviation.

An attempt was made to refine the scale factors using the set of transferable scale factors recommended by Pulay *et al.* [18]. Vibrational frequencies calculated at HF/6-311G and B3LYP/6-311G levels were scaled by 0.8821 for wavenumbers less than 1700 cm^{-1} and 0.9811 for higher wavenumbers.

The vibrational assignments in the present work are based on the HF/6-311G and B3LYP/6-311G frequencies, infrared intensities, Raman activities as well as characteristic group frequencies. The detailed vibrational assignments of fundamental modes of HDMP along with observed and calculated frequencies, and normal mode descriptions have been reported in Table 3. It is convenient to discuss the vibrational spectra of HDMP in terms of characteristic spectral region as describe below:

O–H vibration
The band at 3330 cm^{-1} in HF/6-311G method and 3322 cm^{-1} in B3LYP/6-311G are assigned to solely to the O–H stretching vibrations as the PEDs shows 98% contributions

in HDMP. Normally, free O–H stretching vibrations appear around 3600 cm^{-1} as in, for example phenol [19]. In the present work shows excellent agreement with experimental values. The weak and very weak intensity band at 3325 cm^{-1} in FT-IR spectra are assigned to O–H stretching vibration. The bands for O–H in-plane bending vibrations of the title compound are identified at 1663 cm^{-1} in HF/6-311G and 1650 cm^{-1} in B3LYP/6-311G. The strong band observed at 1651 cm^{-1} in FT-IR spectrum is assigned to O–H in-plane bending vibration of HDMP. The same vibrations appear in the FT-Raman spectra at 1651 cm^{-1} with medium intensity for HDMP. The O–H out-of-plane bending vibrations of HDMP are observed strong band at 836 cm^{-1} in FT-IR spectrum and weak band 831 cm^{-1} in FT-Raman spectrum. These assignments are also supported by the literature.

C–H vibration

The hetero aromatic organic compounds and its derivatives are structurally very close to benzene and commonly exhibit multiple weak bands in the region 3100–3000 cm^{-1} due to C–H stretching vibrations [20–22]. The aromatic C–H stretching vibrations are observed in the region 3152 cm^{-1} in FT-IR spectrum and the computed values at 3172 cm^{-1} in HF/6-311G and 3153 cm^{-1} in B3LYP/6-311G methods are assigned to C–H stretching vibration. These assignments are in line with the literature and further in this region, the bands not much affected due to the nature and position of the substitution. The C–H in-plane bending vibrations normally occur as a number of strong to weak intensity sharp bands in the region 1300–1000 cm^{-1} [23]. The bands for C–H in-plane bending vibration of the title compound are identified at 1214 cm^{-1} in HF/6-311G and 1205 cm^{-1} in B3LYP/6-311G methods. The corresponding vibrations are also observed at strong band 1207 cm^{-1} in FT-Raman spectrum of HDMP, respectively, by our calculation are assigned to C–H in-plane bending vibrations, which coincide with experimental values.

The C–H out-of-plane bending vibrations are strongly coupled vibrations and occur in the region 900–667 cm^{-1} [24–27]. In the present case, the C–H out-of-plane bending vibration of the title compound are found at 885 cm^{-1} in HF/6-311G and 872 cm^{-1} in B3LYP/6-311G methods. The corresponding vibrations are also observed weak band at 873 cm^{-1} in FT-Raman spectrum of HDMP. The in-plane and out-of-plane bending vibrational frequencies are found to be well within their characteristic regions. This shows that the substitution of OH and CH$_3$ do not affect much of aromatic C–H modes of vibration as they attached to only carbon of the benzene ring.

CH$_3$ Vibrations

The title molecule under consideration possesses two CH$_3$ group in the side substituted chain. For the assignments of CH$_3$ group frequencies one can expect that nine fundamentals can be associated to each CH$_3$ group. These vibrations are CH$_3$ ss (symmetric Stretching), CH$_3$ ips (in-plane stretching), CH$_3$ ipb (in-plane bending), CH$_3$ sb (symmetric bending), CH$_3$ ipr (in-plane rocking), CH$_3$ opr (out-of-plane rocking), tCH$_3$ (twist), CH$_3$ops (out-of-plane stretching), CH$_3$opb (out-of-plane bending) vibrations, respectively. Methyl groups are generally referred as electron donating substituent's in the aromatic ring system.

The C–H methyl group stretching vibrations are highly localized and generally observed in the range 3000–2800 cm^{-1} [28, 29]. In the present investigation, the bands with sharp peaks are found at 3106, 3075, 3029, 2971, 2943, 2895 cm^{-1} in HF/6-311G and 3080, 3064, 3014, 2955, 2933, 2870 cm^{-1} in B3LYP/6-311G are assigned CH$_3$ asymmetry and symmetry stretching vibrations. For HDMP, the values observed at 3065, 2956, 2934 cm^{-1} in FT-IR spectrum and 3083, 3014, 2955, 2928 cm^{-1} FT-Raman spectrum are assigned to CH$_3$ stretching vibrations. The computed values found at 667, 649, 758, 722 cm^{-1} in HF/6-311G and 652, 637, 740, 709 cm^{-1} in B3LP/6-311G are assigned to CH$_3$ in-plane rock and out-of-plane rock of HDMP molecule. The recorded FT-IR spectrum medium to weak band observed at 738, 710 cm^{-1} and three weak bands observed at 654, 638, 748 cm^{-1} in FT-Raman spectra are assigned to CH$_3$ in-plane rock and out-of-plane rock of HDMP. The B3LYP method also shows good agreement with observed values of HDMP.

The asymmetrical CH$_3$ deformation vibrations are computed at 1466, 1148, 1052, 970 cm^{-1} in HF/6-311G and 1455, 1136, 1042, 960 cm^{-1} in B3LYP/6-311G for HDMP. Similarly, the symmetrical CH$_3$ deformation vibrations are computed at 1433, 952 cm^{-1} in HF/6-311G and 1426, 940 cm^{-1} in B3LYP/6-311G for HDMP. These fundamental values show good agreement with the observed strong to medium band at 1453, 962, 1422 cm^{-1} FT-IR and medium band 1455, 1138, 1041, 955, 1428, 941 cm^{-1} in FT-Raman. The computed values at 57, 40 cm^{-1} and 59, 32 cm^{-1} are assigned to CH$_3$ twisting vibrations by both HF/6-311G and B3LP/6-311G methods, respectively. This assignment is also supported by the literature.

C=O vibration

The absorption is sensitive for both the carbon and oxygen atoms of the carbonyl group. Both have the same while it vibrates. Normally carbonyl group vibrations occur in the region 1780–1680 cm^{-1} [30–32]. In the present study, the C=O stretching vibration is assigned at 1195 cm^{-1} in HF/6-311G method and 1180 cm^{-1} in B3LYP/6-311G method. According to the literature, the C=O vibration is pushed to the lower region by the influence of other vibrations, because of the proximity. Hence, the present investigation, the strong FT-IR band is observed at 1181 cm^{-1}. The C=O in–plane bending vibration is usually found at 700 cm^{-1}[33, 34]. In HDMP, the C=O in-plane bending vibration is found at 934 cm^{-1} in HF/6-311G and 923 cm^{-1} in B3LYP /6-311G, which is found mixed with the O–H deformation mode. In HDMP, the observed medium band at 920 cm^{-1} in FT-IR spectrum and weak band observed at 928 cm^{-1} in FT-Raman spectrum are assigned to C=O in-plane bending vibration. The C=O out-of-plane bending vibration is expected in the region 540±80 cm^{-1} [35]. A medium C=O out-of-plane bending vibration is found at 856 cm^{-1} in B3LYP/6-311G and it is also observed weak band at 858 cm^{-1} in both FT-IR and FT-Raman spectra. According to the literature, this assigned value is slightly above the expected range. From the above observation, it is clear that, the C=O vibration is not influenced by the other substitution in the chain.

C–C vibration

The ring C=C and C–C stretching vibrations, known as semicircle stretching usually occur in the region 1400–1625 cm^{-1} [36]. The C–C stretching peaks found at 1675, 1480, 633, 564 cm^{-1} in HF/6-311G and 1663, 1472, 624, 554 cm^{-1} in B3LYP/6-311G method are assigned to C–C stretching vibrations. The bands observed at 1661, 626, 556 cm^{-1} in FT-IR spectrum and 1666, 1469, 624, 555 cm^{-1} in FT-Raman spectrum are assigned to C–C stretching vibrations in HDMP molecule. According to the literature, C–C stretching vibrations are found to be well within their characteristic regions.

In the present work, the computed three strong bands present at 545, 482 cm^{-1} in HF/6-311G and 532, 470 cm^{-1} in B3LYP/6-311G are assigned to C–C in-plane bending vibrations. The band observed at 306 cm^{-1} in FT-Raman spectrum is assigned to C–C out-of-plane bending vibrations in HDMP molecule. These assignments are in line with the literature [29].

C–N vibration

The quinoline and its related compounds show a strong absorption band in the region 1600–1500 cm^{-1} due to C=N stretching vibration [36]. The observation in the present work shows the presence of C=N stretching vibrations at 1635, 1399, 1315, 856 cm^{-1} in HF/6-311G and 1624, 1388, 1304, 847 cm^{-1} in B3LYP/6-311G methods. These bands have strong to medium intensity and these are slightly lower than the expected value. The strong intensity of the band may due to the mixing of C=N with C=C, both occurring at the same frequency. The C–N stretching vibrations are always mixed with other bands and normally occur in the region 1266–1382 cm^{-1} [35, 23, 29, 37-39]. For HDMP, the C–N in-plane vibrations are observed at 1621, 1393, 1302 cm^{-1} in FT-IR spectrum and 1624, 1386 cm^{-1} in FT-Raman spectrum, which is in close agreement with the literature value.

4.3 Computed IR intensity and Raman activity analysis

Computed vibrational spectral IR intensities and Raman activities of the corresponding wavenumbers by HF/6-311G and B3LYP/6-311G methods have been displayed in the Table 4. Comparison of the IR intensities and Raman activities calculated by B3LYP/6-311G with experimental values exposes the variation in IR intensities and Raman activities. These variations are due to the absence of electrons correlation in HF method.

4.4 Vibrational force constant

The output files of the quantum mechanical calculations contain the force constant matrix in Cartesian coordinates and in Hartree/Bohr^2 units. These force constants were transformed to force fields in the internal local symmetry coordinates. The force field determined was used to calculate the vibrational potential energy distribution among the normal coordinate. In both methods, the values show the variation due to the inclusion of electron correlation in B3LYP method. They are listed in Table 4.

4.5 Mulliken population analysis: Mulliken Atomic Charges

Mulliken atomic charge calculation [40] has an important role in the application of quantum chemical calculation to molecular system, because the atomic charges affect dipole moment, polarizability, electronic structure, and much more properties of molecular systems. The total atomic charges of HDMP obtained by Mulliken population analysis with both HF/6-311G and B3LYP/6-311G methods are listed in Table 5.

For HF/6-311G and B3LYP/6-311G methods, the Mulliken atomic charge of C4 atom occupies the higher positive value and becomes highly acidic. Their corresponding Mulliken atomic charges are 0.678 in HF/6-311G and 0.567 in B3LYP/6-311G method. This value was higher than other carbon atoms. The H13 atom have low value compare to other hydrogen atoms (H8, H9, H10, H15, H16, H16) due to the formation of intramolecular weak hydrogen bonding O–H…H.

4.6 HOMO-LUMO analysis

The analysis of the wave function indicates that the electron absorption corresponds to the transition from the ground to the first excited state and is mainly described by one electron excitation from the highest occupied molecular orbital (HOMO) to the lowest unoccupied molecular orbital (LUMO). The LUMO of p nature (i.e. benzene ring) is delocalized over the whole CC bond. By contrast, the HOMO is located over methoxy and hydroxyl groups; consequently the HOMO–LUMO [41] translation implies an electron density transfer to aromatic part of benzaldehyde of p conjugated system from hydroxyl groups. Moreover, these orbital significantly overlap in their position for HDMP. On the basis of fully optimized ground state structure, B3LYP/6-311G calculations have been used to determine the low lying excited states of HDMP. The calculated results involving the vertical excitation energies, oscillator strength and wavelengths are carried out and compared with measured experimental wavelength. The HOMO – LUMO energy gap of HDMP was calculated at the HF/6-311G and B3LYP/6-311G level and are shown Table 6 reveals that the energy gap reflect the chemical activity of the molecule. LUMO as an electrons acceptor represents the ability to obtain an electron represents the ability to donate an electron. The calculated HOMO–2 from LUMO+2, energy gap is lower than the other orbital of the molecular system. The electron transfer occurs only in this orbital, the plots of molecular orbitals are shown in Fig. 4.

4.7 Hyperpolarizability

The first hyperpolarizabilities (β_{total}) of this novel molecular system, and related properties (β, α_0 and α) of HDMP were calculated using B3LYP/6-311G basis set, based on the finite-field approach. In the presence of an applied electric field, the energy of a system is a function of the electric field. Polarizabilities and hyperpolarizabilities characterize the response of a system in an applied electric field [42]. They determine not only the strength of molecular interactions (long-range inter induction, dispersion force,

etc.) as well as the cross sections of different scattering and collision process and also the nonlinear optical properties (NLO) of the system [43, 44]. First hyperpolarizability is a third rank tensor that can be described by 3×3×3 matrix. The 27 components of the 3D matrix can be reduced to 10 components due to the Kleinman symmetry [43]. The components of first hyperpolarizability (β_{total}) are defined as the coefficients in the Taylor series expansion of the energy in the external electric field. When the external electric field is weak and homogeneous, this expansion becomes:

$$E = E^0 - \mu_\alpha F_\alpha - 1/2 \alpha_{\alpha\beta} F_\alpha F_\beta - 1/6 \beta_{\alpha\beta\gamma} F_\alpha F_\beta F_\gamma + \cdots$$

$$\ldots(3)$$

where E^0 is the energy of the unperturbed molecules, F_α the field at the origin μ_α, $\alpha_{\alpha\beta}$ and $\beta_{\alpha\beta\gamma}$ are the components of dipole moments, polarizability and the first hyperpolarizabilities, respectively. The total static dipole moments μ, the mean polarizabilities α_0, the anisotropy of the polarizabilities α and the mean first hyperpolarizabilities β_{total}, using the x, y and z components they are defined as: [43, 45].

The total static dipole moment is

$$\mu = \sqrt{\left(\mu_x^2 + \mu_y^2 + \mu_z^2\right)} \qquad \ldots(4)$$

The isotropic polarizability is

$$\alpha_o = \frac{\alpha_{xx} + \alpha_{yy} + \alpha_{zz}}{3} \qquad \ldots(5)$$

The polarizability anisotropy invariant is

$$\alpha = 2^{\frac{1}{2}}\left[\left(\alpha_{xx} - \alpha_{yy}\right)^2 + \left(\alpha_{yy} - \alpha_{zz}\right)^2 + \left(\alpha_{zz} - \alpha_{xx}\right)^2 + 6\alpha_{xx}^2\right]$$

$$\ldots(6)$$

and the average hyperpolarizability is

$$\beta_{total} = \sqrt{\left(\beta_x^2 + \beta_y^2 + \beta_z^2\right)} \qquad \ldots(7)$$

$$\beta^{vec} = 3/5\left[\left(\beta_x^2 + \beta_y^2 + \beta_z^2\right)^{1/2}\right] \qquad \ldots(8)$$

and

$$\beta_x = \beta_{xxx} + \beta_{xyy} + \beta_{xzz}$$
$$\beta_y = \beta_{yyy} + \beta_{xxy} + \beta_{yzz}$$
$$\beta_z = \beta_{zzz} + \beta_{xxz} + \beta_{yyz}$$

The B3LYP/6-311G method calculated the first order hyperpolarizability of HDMP is 6.4075×10^{-31} esu. The total molecular dipole moment (μ), mean polarizability (α_o) and anisotropy polarizability ($\Delta\alpha$) and first hyperpolarizability (β_{total}) of HDMP are computed and are depicted in Table 7.

4.8 Electrostatic potential

Molecular electrostatic potential (ESP) at a point in the space around a molecule gives an indication of the net electrostatic effect produced at that point by the total charge distribution (electron + nuclei) of the molecule and correlates with dipole moments, electronegativity, partial charges and chemical reactivity of the molecules. It provides a visual method to understand the relative polarity of the molecules. An electron density isosurface mapped with electrostatic potential surface depicts the size, shape, charge density and site of chemical reactivity of the molecules.

The different values of the electrostatic potential represented by different colors; red represents the regions of the most negative electrostatic potential, blue represents the regions of the most positive electrostatic potential and green represents the region of zero potential. Potential increases in the order red < orange < yellow < green < blue. Such mapped electrostatic potential surfaces have been plotted for title molecules in B3LYP/6-311G basis set using the computer software GAUSSVIEW[9]. Projections of this surface along the molecular plane and a perpendicular plane are given in Fig. 5 for HDMP. This Figure provides a visual representation of the chemically active sites and comparative reactivity of atoms.

It may see that, in both the molecules, a region of zero potential envelopes the π-system of the aromatic rings, leaving a more electrophilic region in the plane of hydrogen atoms. The shapes of the electrostatic potential at sites close to the polar group in the two molecules. The halogen group in the molecules is influenced by the stereo structure and the charge density distribution. These sites show regions of most negative electrostatic potential and high activity of the halogen groups. In contrast, regions close to the other polar atom-oxygen of the aromatic ring show regions of mildly negative and zero potential, respectively [46].

4.9 Natural Bond Orbital analysis

Hyper conjugation is an important effect in which an occupied Lewis-type NBO is stabilized by overlapping with a non-Lewis type orbital. This electron delocalization can be described as a charge transfer from a Lewis valence orbital with a decrease in its occupancy, to a non-Lewis. Several other types of valuable data, such as directionality, hybridization, and partial charges, have been analyzed from the NBO results [27, 28].

In Table 8, BD(1)N1–C2 orbital with 1.9864 electrons has 59.5% N1 character in a $sp^{1.78}$ hybrid and has 40.5% C2 character in a $sp^{2.0}$ hybrid. The $sp^{1.63}$ hybrid on N has 64.02% p–character and the $sp^{2.10}$ hybrid on C has 70.16% p-character in HF method. For B3LYP method, the BD(1)N1–C2 orbital with 1.9888 electrons has 59.9% N1 character in a $sp^{1.69}$ hybrid and has 40% C2 character in a $sp^{2.1}$ hybrid. The $sp^{1.9}$ hybrid on N has 65.51% p-character and the $sp^{2.0}$ hybrid on C has 67.9% p-character. An idealized sp^2 hybrid has 75% p-character. The four coefficients 0.7714, 0.6364, 0.774, and 0.633 are called polarization coefficients of HDMP in both HF and B3LYP methods, respectively. The sizes of these coefficients show the importance of the two hybrids in the formation of the bond. In both molecule the nitrogen has larger percentage of NBO and gives the larger polarization coefficient because it has the higher electronegativity. Similar results are found in all the BD (1) C–N orbital's.

Perturbation theory energy analysis
Delocalization of the electron density between occupied Lewis type (bond (or) lone pair) NBO orbital's and formally unoccupied (antibond (or) Rydberg) non Lewis NBO

orbital's corresponding to a stabilizing donor-acceptor interaction. The energy of this interaction can be estimated by the second order perturbation theory [16]. Table 9 lists the calculated second order interaction energies ($E^{(2)}$) between the donor-acceptor orbital's in HDMP molecule.

The important interaction energies are 3.25, 4.67, 4.28, 13.17, 12.19 kcal/mol in HF/6-311G method and 2.34, 3.4, 3.77, 2.86, 3.03 kcal/mol in B3LYP/6-311G method. These values are identified at BD(1)N1–C2, BD(1)C2–C7, BD(1)C4–C5, LP(1)N1, LP(1)N3 donor NBOs and their corresponding acceptors NBOs are BD*(1)C2–C7, BD*(1)N1–C6, BD*(1)C5–C6, BD*(1)C2–N3, BD*(1)N1–C2, respectively. These differences in interaction energies are due to the substitution of atoms like N, OH and CH_3, respectively. By comparing HF and B3LYP methods, the HF energy values are higher than B3LYP energy values. These variations are due to the neglect of electron correlation.

5. Conclusion

The present investigation thoroughly analyzed the conformational stability, HOMO–LUMO, NBO and the vibrational spectra, both infrared and Raman of HDMP molecule with HF/6-311G and B3LYP/6-311G methods. All the vibrational bands observed in the FT-IR and FI-Raman spectra of these compounds are assigned to the various modes of vibration and most of the modes have wavenumbers in the expected range. The complete vibrational assignments of wavenumbers are made on the basis of potential energy distribution (PED). The scaled B3LYP/6-311G results are the best over the HF/6-311G methods. The electrostatic potential surfaces (ESP) together with complete analysis of the vibrational spectra, both IR and Raman and electronic spectra help to identify the structural and symmetry properties of the title molecule. The excellent agreement of the calculated and observed vibrational spectra reveals the advantages of higher basis set for quantum chemical calculations. NBO analysis provides an efficient method for studying inter and intra molecular interaction in molecular system. The stabilization energy has been calculated from second order perturbation theory. The NBO analysis confirms the hyper conjugation interaction. The strengthening and increase in wave number is due to the hyper conjugation interaction. Natural Bond Orbital analysis shows the differences in interaction of energies are due to the substitution of N, OH and CH_3 groups, respectively. Finally the calculated HOMO and LUMO energies shows that charge transfer occur in the molecules, which are responsible for the bioactive property of the biomedical compound HDMP. Thermodynamic analysis reveals that all the thermodynamic parameters calculated are directly proportional to temperature.

References

[1] N. Sungaraganesan, K. Sathes Kumar, C. Meganathan, Spectrochim. Acta 65A (2006) 1186.
[2] K. Balci, S. Akyuz, J. Mol. Struct, 744−747 (2005) 909.
[3] M. K. Subramanian, P. M. Anbarasan, S. Manimegalai, Spectrochim. Acta 73A (2009) 642.
[4] M.J. Frisch, G.W. Trucks, H.B. Schlegal, G.E. Scuseria, M.A. Robb, J.R. Cheesman, V.G. Zakrzewski, J.A. Montgomerg, Jr., R.E. Strtmann, J.C. Burant, S. Dapprich, J.M. Milliam, A.D. Daniels, K.N. Kudin, M.C. Strain, O. Farkas, J. Tomasi, V. Barone, M. Cossi, R. Camme, B. Mennucci, C. Pomelli, C. Adamo, S. Clifford, J. Ochterski, G.A. Petersson, P.Y. Ayala, Q. Cui, K. Morokuma, N. Rega, P. Salvador, J.J. Dannenberg, D.K. Malich, A.D. Rabuck, K. Raghavachari, J.B. Foresman, J. Cioslowski, J.V. Ortiz, A.G. Baboul, B.B. Stetanov, G. Liu, A. Liashenko, P. Piskorz, I. Komaromi, R. Gomperts, R.L. Martin, D.J. Fox, T. Keith, M.A. Al- Laham, C.Y. Peng, A. Nsnsyskkara, M. Challacombe, P.M.W. Gill, B. Johnson, W. Chen, M.W. Wong, J.L. Andres, C. Gonzalez, M. Head-Gordon, E.S. Replogle and J.A. Pople, *GAUSSIAN09, Revision A.02, Gaussian*, Inc, Pittsburgh, 2009.
[5] T. Sundius, J. Mol. Struct., 218(1990) 321.
[6] (a) T. Sundius, Vib.Spectrosc., 29 (2002) 89;
[7] (b) Molvib,V.7.0: Calculation of Harmonic Force Fields and Vibrational modes of molecules, QCPE Program No.807(2002).
[8] A.D. Becke, J. Chem. Phys., 98 (1993) 5648.
[9] C. Lee, W. Yang, R.R. Parr, Phys. Rev. B 37 (1988) 785.
[10] M.J.Frisch, A.B.Nielson, A.J.Holder, *Gaussview Users Manual, Gaussian Inc.*, Pittsburgh, PA, 2008.
[11] G. Keresztury, S. Holly, J. Varga, G.Besenyei, A.Y. Wang, J.R. Durig, Spectrochim. Acta 49A (1993) 2007.
[12] G. Keresztury,J.M. Chalmers, P.R. Griffith (Eds.), Raman Spectroscopy: Theory, Handbook of Vibrational Spectroscopy, Vol. 1, John Wiley & Sons Ltd., New York, 2002.
[13] A. E. Reed, F. Weinhold, J. Chem.Phys., 83 (1985) 1736.
[14] M. Snehalatha, C. Ravikumar, I . Hubert Joe, V.S. Jayakumar, J. Raman Spectrosc. 40 (2009) 1121.
[15] I. Hubert Joe, Irena Kostova, C. Ravikumar, M. Amalanathan, Simona Cinta Pinzaru, J. Raman Spectrosc. 40 (2009) 1033.
[16] A.E. Ledesma, J. Zinczuk, A. Ben Altabef, J. J. Lopez Gonzalez, S. A. Brandan, J. Raman Spectrosc. 40 (2009) 1004.
[17] J. Chocholousova, V. Vladimir Spirko, P. Hobza, Phys. Chem. Chem. Phys. 6 (2004) 37.
[18] S. Melandri, M.E. Sanz, W. Caminali, P.G. Favero, Z. Kisiel, J.Am. Chem. Soc. 120 (1998) 11504.
[19] P. Pulay, G. Fogarasi, F. Pongor, J. E. Boggs, J. Am. Chem. Soc., 101 (1979) 2550.
[20] H. Lampert, W. Mikenda, A. Karpten, J. Phys. Chem., A 101 (1997) 2254.
[21] V. Krishnakumar, V. Balachandran, T. Chithambranathan, Spectrochim. Acta 62A (2005) 918.
[22] W. O. George, P. S. Mcintyre, Infrared Spectroscopy, JohnWiley & Sons , London, 1987.
[23] V. Balachandran, A. Lakshmi, A. Janaki, Spectrochim. Acta 81A (2011) 1.
[24] G. Socrates, Infrared and Raman Characteristic group frequencies, third ed.,Wiley New York, 2001.
[25] V. Krishnakumar, R. John Xavier, Indian J. Pure Appl. Phys., 41 (2003) 597.

[26] V. Krishnakumar, V. N. Prabavathi, Spectrochim. Acta 71A (2008) 449.

[27] A. Altun, K. Golcuk, M. Kumru, J Mol. Struc., (Theochem) 637(2003) 155−169.

[28] V. Karunakaran, V. Balachandran, Spectrochim. Acta 98A (2012) 229.

[29] F. R. Dollish, W. G. Fateley, F. F. Bentely, Characteristic Raman Frequencies on Organic Compounds, Wiley, New York,1997.

[30] R. M. Silverstein, G. Clayton Bassler, T. C. Morril, Spectroscopic Identification of Organic Compounds, John Wiley, New York, 1991.

[31] R. L. Peesole, L. D. Shields, I. C. The Cairus, McWilliam, Modern Method of Chemical Analysis, Wiley, NewYork, 1976.

[32] V. Balachandran, S. Rajeswari, S. Lalitha, J. Mol. Struct. 1007 (2012) 63.

[33] A. Borba, M. Albrecht, A. Gomez–Zavaglia, L. Lapinski, M. J. Nowak, M. A. Suhm, R. Fausto, Phys. Chem. Chem. Phys. 10 (2008) 7010.

[34] J. Mohan, Organic Spectroscopy–Principle and Applications, 2nd ed., Narosa Publishing House, NewDelhi,2000, PP. 30.

[35] V. Krishnakumar, R. John Xavier, T. Chithambaranathan, Spectrochim. Acta 62A (2005) 931.

[36] N. P. G.Roges, A. Guide to the interpretation of Infrared Spectra of Organic Structures, Wiley, NewYork,1994.

[37] G. Varsanyi, Vibrational Spectra of Benzene Derivatives, Academic Press, NewYork, 1969.

[38] M. Robert, G. Cleyton Basseler, T.C. Morrill, Spectrometric Identification of Organic Compounds, John Wiley & Sons ,Singapore,1981.

[39] D. P. Dilella, H. D. Stidham, J. Raman Spectrosc. 9 (1980) 90.

[40] V. Balachandran, S. Lalitha, S. Rajeswari, Spectrochim. Acta 97A (2012) 1023.

[41] V. K. Rastogi, M. A. Palafox, L. Mittal, N. Peica, W. Kiefer, k. Lang, P. Ohja, J. Raman Spectrosc., 38 (2007) 122.

[42] D. Arul Dhas, I. Hubert Joe, S.D.D. Roy, T.H. Freeda, Spectrochim. Acta Part A 77 (2010) 36.

[43] C.R. Zhang, H.S. Chen, G.H. Wang, Chem. Res. Chinese. U. 20 (2004) 640.

[44] Y. Sun, X. Chen, L. Sun, X. Guo, W. Lu, J. Chem. Phys. Lett. 381 (2003) 397.

[45] O. Christiansen, J. Gauss, J.F. Stanton, J. Chem. Phys. Lett. 305 (1999) 147.

[46] A. Kleinman, J. Phys. Rev. 126 (1962) 1977.

[47] V. P. Gupta, A. Sharma, V. Virdi, J.Raman Spectrochim. Acta Part A 64 (2006) 57.

Table 1: Calculated energies of 4-hydroxy-2,6-dimethylpyrimidine (HDMP) obtained by HF/6-311G and B3LYP/6-311G

Conformers	HF/6-311G	B3LYP/6-311G
C1	−415.526560796	−418.151659083
C2	−415.535660070	−418.159305208

Table 2: Optimized geometrical parameters of 4-hydroxy-2,6-dimethyl pyrimidine (HDMP) obtained by HF/6-311G and B3LYP/6-311G density functional calculations

Parameters	Expt. Value[a]	Calculated Values (Å)		Parameters	Expt. value[a]	Calculated Values (°)	
		HF	**DFT**			**HF**	**DFT**
N1–C2		1.32	1.35	C2–N1–C6	116	119	118
N1–C6	1.34	1.31	1.34	N1–C2–N3	127	123	124
C2–N3	1.33	1.32	1.35	N1–C2–C7		119	119
C2–C7	1.34	1.49	1.50	N3–C2–C7		118	117
N3–C4		1.32	1.33	C2–N3–C4	116	118	117
C4–C5	1.33	1.38	1.39	N3–C4–C5	123	122	123
C4–O11	1.39	1.35	1.37	N3–C4–O11		118	118
C5–C6		1.38	1.39	C5–C4–O11		119	119
C5–H13		1.07	1.08	C4–C5–C6	116	118	116
C6–C14		1.49	1.50	C4–C5–H13		121	121
C7–H8		1.08	1.09	C6–C5–H13		123	123
C7–H9		1.08	1.09	N1–C6–C5	123	120	122
C7–H10		1.08	1.09	N1–C6–C14		116	116
O11–H12		0.95	0.98	C5–C6–C14		123	123
C14–H15		1.08	1.09	C2–C7–H8		110	110
C14–H16		1.08	1.09	C2–C7–H9		110	110
C14–H17		1.08	1.09	C2–C7–H10		110	110
				H8–C7–H9		107	107
				H8–C7–H10		109	109
				C7–H9–H10		109	109
				C4–O11–H12		112	109
				C6–C14–H15		110	110
				C6–C14–H16		112	112
				C6–C14–H17		110	110
				H15–C14–H16		109	109
				H15–C14–H17		107	107
				H16–C14–H17		109	109

ᵃ Taken from Ref. [17].
For numbering of atom refer Fig. 3

Table 3: Assignment of fundamental vibration of 4-hydroxy-2,6-dimethyl pyrimidine (HDMP) by normal mode analysis based on SQM force field calculations by HF/6-311G and B3LYP/6-311G force fields.

Mode	FT-IR	FT-Raman	unscaled		scaled		Assignments/(PED%)
			HF	B3LYP	HF	B3LYP	
A′	3325(w)		4056	3648	3330	3322	νOH(98)
A′	3152(w)		3409	3226	3172	3153	νCH(98)
A′		3083(m)	3295	3148	3106	3080	ν_{as} CH₃ (99)
A′	3065(w)		3261	3117	3075	3064	ν_{as} CH₃ (99)
A′		3014(m)	3245	3091	3029	3014	ν_{as} CH₃ (98)
A′	2956(m)	2955(m)	3240	3088	2971	2955	ν_{as} CH₃ (98)
A′	2934(s)	2928(s)	3183	3033	2943	2933	ν_{ss} CH₃ (98)
A′	2869(m)		3180	3030	2895	2870	ν_{ss} CH₃ (99)
A′	1661(s)	1666(m)	1788	1632	1675	1663	νCC(74), βCO(18)
A′	1651(s)	1651(s)	1749	1587	1663	1650	βOH(62), νCO(18)
A′	1621(s)	1624(m)	1640	1523	1635	1624	νCN(88)
A′		1469(s)	1634	1520	1480	1472	νCC(68), βCH(22)
A′	1453(s)	1455(m)	1632	1519	1466	1455	δad CH₃ (86)
A′	1422(m)	1428(m)	1630	1515	1433	1426	δsd CH₃ (85)
A′	1393(m)	1386(m)	1595	1459	1399	1388	νCN(88)
A′	1302(m)		1585	1453	1315	1304	νCN(68)
A′		1207(s)	1573	1449	1214	1205	βCH (78), νCC(14)
A′	1181(s)		1565	1425	1195	1180	νCO(68), νCC(24)
A′		1138(m)	1540	1411	1148	1136	δad CH₃ (96)
A′		1041(m)	1370	1278	1052	1042	δad CH₃ (94)
A″	962(m)	955(m)	1297	1211	970	960	δad CH₃ (83)
A″		941(m)	1256	1178	952	940	δsd CH₃ (86)
A′	920(m)	928(w)	1205	1102	934	923	βCO (76), γOH (22)
A′		873(w)	1198	1094	885	872	γCH (82)
A″	858(w)	858(w)	1176	1084	867	856	γCO(46),γCC(28)
A″			1150	1071	856	847	νCN(72)
A″	836(s)	831(w)	1082	1004	842	833	γOH (88)
A′	738(m)	748(w)	1054	962	758	740	γ CH₃ op roc (88), νCC (12)
A′	710(w)		1036	954	722	709	γ CH₃ op roc (75), νCC(13)
A′		654(w)	965	883	667	652	γ CH₃ ip roc (76)
A″		638(w)	872	787	649	637	γ CH₃ ip roc (78)
A′	626(m)	624(s)	725	656	633	624	νCC(72), β ring(13)
A′	577(s)	569(m)	658	614	585	571	β ring(52), νCC(18)
A″	556(s)	555(m)	634	575	564	554	νCC(61), β ring(13)
A′	535(m)		609	568	545	532	βCC(62). βCO (26)
A′	507(s)	514(m)	593	563	526	510	β ring(67), νCC(15)
A′	472(w)		570	552	482	470	βCC (68),γCC(12)
A′	446(w)	456(w)	544	504	463	450	β ring (72), γCC(17)
A″			337	314	325	323	γCC(62), β ring (13)
A″		306(m)	318	316	315	306	γCC(63), β ring(11)
A″		237(m)	267	254	244	235	γ ring(56), γCC(26)
A″		210(w)	225	197	212	208	γ ring(54), γCH(14), νCC(11)
A″		114(w)	207	184	124	113	γ ring(58), γCC(18)
A″			84	58	57	59	τ CH₃ (76)
A″			62	47	40	32	τ CH₃ (74)

ν_{as}-asymmtric stretching, ν_{ss}-symmtric stretching ν-stretching, β-in-plane bending, γ-out-of-plane bending, δad –asymetric deformation, ip roc-in plane rocking, op roc-out of plane rocking, τ-twisting

Table 4: Reduced mass, Force constant, IR intensities and Raman activities of 4-hydroxy-2,6-dimethyl pyrimidine (HDMP)

Reduced mass		Force constant		IR intensity		Raman activity	
HF	B3LYP	HF	B3LYP	HF	B3LYP	HF	B3LYP
1.07	1.06	10.33	8.34	118.93	56.85	92.36	161.20
1.10	1.09	7.50	6.71	1.28	3.32	83.81	102.89
1.10	1.10	7.03	6.41	13.27	9.78	55.37	56.02
1.10	1.10	6.90	6.30	25.71	20.68	62.52	63.34
1.10	1.10	6.82	6.18	17.51	13.27	78.86	85.58

1.10	1.10	6.80	6.17	20.41	14.75	84.36	93.58
1.04	1.04	6.20	5.63	13.41	10.03	182.79	215.99
1.04	1.04	6.17	5.60	16.96	13.14	144.84	176.59
6.11	5.30	11.52	8.31	348.95	222.60	8.78	7.14
6.31	4.19	11.38	6.21	382.24	196.75	14.03	15.08
1.23	1.16	1.94	1.59	106.76	97.13	9.55	12.09
1.05	1.05	1.64	1.42	8.04	9.56	16.68	16.05
1.12	1.13	1.75	1.54	19.68	36.27	7.69	13.18
1.05	1.05	1.64	1.41	11.98	13.48	14.18	13.40
2.54	1.62	3.80	2.03	54.54	17.09	4.60	24.34
2.03	1.34	3.00	1.67	19.36	51.77	10.00	15.35
2.43	3.64	3.54	4.50	32.45	82.13	5.49	2.57
1.62	3.12	2.34	3.73	0.42	31.78	4.75	2.67
2.21	3.07	3.08	3.60	19.03	12.51	0.40	2.47
1.79	2.48	1.98	2.39	97.95	72.46	1.58	3.67
1.82	3.04	1.80	2.63	98.67	9.63	2.58	3.17
2.66	1.51	2.47	1.23	154.79	240.89	3.10	0.34
1.61	1.59	1.38	1.13	0.15	0.03	0.93	0.41
1.65	1.61	1.40	1.13	15.29	11.64	0.35	0.15
1.98	2.12	1.62	1.47	0.74	3.33	2.53	2.54
1.95	1.78	1.52	1.21	0.83	4.11	2.84	0.71
5.03	4.38	3.47	2.60	8.92	5.08	10.50	11.25
3.70	4.75	2.42	2.59	9.59	5.98	4.79	6.39
3.32	2.89	2.10	1.55	28.51	39.27	0.10	0.25
1.62	1.46	0.89	0.67	49.31	19.89	0.31	0.04
2.86	3.69	1.28	1.35	12.29	6.84	0.25	0.36
4.28	4.12	1.33	1.04	7.05	16.09	0.86	0.99
4.66	4.65	1.19	1.03	7.12	5.95	18.27	17.41
3.07	2.24	0.73	0.44	5.00	45.90	1.04	2.47
6.66	1.34	1.46	0.25	4.40	99.88	5.58	2.32
5.38	6.66	1.12	1.24	12.17	2.01	6.31	5.89
1.12	5.51	0.21	0.99	191.45	9.41	2.66	5.06
3.26	3.21	0.57	0.48	19.58	15.96	0.16	0.11
3.52	3.55	0.24	0.21	4.94	5.54	0.56	1.22
2.52	2.50	0.14	0.12	2.90	2.33	0.69	1.27
8.94	9.11	0.38	0.29	1.91	1.47	0.42	0.19
3.35	3.36	0.10	0.08	2.78	5.14	1.87	0.96
3.25	3.31	0.08	0.07	2.91	0.38	0.44	1.24
1.04	1.03	0.00	0.00	0.46	0.64	0.13	0.18
1.03	1.03	0.00	0.00	0.62	0.79	0.22	0.31

Table 5: Mulliken atomic charges of 4-hydroxy-2,6-dimethyl pyrimidine (HDMP) obtained by HF/6-311G and B3LYP/6-311G method

Atom	Mulliken atomic charge	
	HF	B3LYP
N1	−0.575	−0.392
C2	0.449	0.282
N3	−0.605	−0.421
C4	0.678	0.567
C5	−0.303	−0.212
C6	0.345	0.215
C7	−0.542	−0.557
H8	0.208	0.211
H9	0.207	0.205
H10	0.210	0.209
O11	−0.739	−0.598
H12	0.419	0.380
H13	0.203	0.184
C14	−0.576	−0.596
H15	0.202	0.206
H16	0.202	0.205
H17	0.218	0.212

Table 6: HOMO-LUMO analysis of 4-hydroxy-2,6-dimethyl pyrimidine obtained by HF/6-311G and B3LYP/6-311G method

Energy	HF/6311+(d, p)	B3LYP/6311+(d, p)
HOMO	−0.40203	−0.28257
HOMO−1	−0.38885	−0.28335
HOMO−2	−0.35732	−0.30532
LUMO	0.06477	−0.11304
LUMO+1	0.07473	−0.05509
LUMO+2	0.08040	−0.04705
HOMO−LUMO energy gap	−0.15642	−0.16953

Table 7: Calculated electric dipole moment (Debye), Polarizability (in a.u), β components and β_{tot} values of 4-hydroxy-2,6-dimethyl pyrimidine by B3LYP/6-311G

Parameters	Value(Debye)	Parameters	Value(Debye)
μ_x	0.4311	β_{xxx}	6.8949
μ_y	−0.2432	β_{xxy}	−4.1498
μ_z	0.0142	β_{yyz}	−0.4464
μ	0.4951	β_{yyy}	14.7171
α_{xx}	−44.5554	β_{xxz}	−0.1520
α_{xy}	−0.8581	β_{xyz}	0.3680
α_{yy}	−55.7895	β_{zzz}	0.6742
α_{xz}	−0.0273	β_{xzz}	−1.2261
α_{zz}	−55.0878	β_{xyy}	19.8647
α_{yz}	−0.0118	β_{yzz}	−1.1040
α_0(esu)	−51.81043	β_{tot}	6.4075×10^{-31}
$\Delta\alpha$(esu)	121.05655×10^{-24}	β^{vec}	3.8445×10^{-31}

Table 8: Natural bond orbital analysis of 4-hydroxy-2,6-dimethyl pyrimidine (HDMP)

| Bond (A-B)	Occupancy		ED_A		ED_B		NBO analysis		S%		p%	
	HF	B3LYP	HF	B3LYP	HF	B3LYP	HF	B3LYP	HF	B3LYP	HF	B3LYP
BD(1) N1-C6	1.9864	1.9888	59.5	59.9	40.5	40.0	$0.771(sp^{1.78})+$ $0.6364(sp^2)$	$0.774(sp^{1.9})+$ $0.633(sp^{2.1})$	35.98 29.84	34.49 32.0	64.02 70.16	65.51 67.9
BD(1)C2-N3	1.9881	1.9849	39.08	59.3	60.92	40.6	$0.625(sp^{2.19})+$ $0.7805(sp^2)$	$0.77(Sp^{1.83})+$ $0.637(sp^{2.3})$	31.3 37.39	35.28 29.6	68.7 62.61	64.72 70.3
BD(1)C2-C7	1.9812	1.9862	51.7	39.3	48.3	60.6	$0.719(sp^{1.73})+$ $0.695(sp^3)$	$0.627(sp^{2.21})+$ $0.778(sp^{1.7})$	36.64 28.08	31.19 36.8	63.36 71.92	68.81 63.1
BD(1)C 4-C5	1.9821	1.9798	49.18	50.9	50.82	49.0	$0.701(sp^{1.43})+$ $0.712(sp^2)$	$0.713(sp^{1.72})+$ $0.7(sp^{2.5})$	41.2 34.23	36.81 27.9	58.8 65.77	63.19 72.0
BD(1)C5-C6	1.9797	1.9815	51.31	49.1	48.69	50.8	$0.716(sp^{1.74})+$ $0.697(sp^2)$	$0.701(sp^{1.4})+$ $0.712(sp^{1.7})$	36.52 36.64	41.67 34.3	63.48 63.36	58.33 65.7
LP(1)N1	1.9477	1.9778					$sp^{2.45}$	$sp^{1.73}$	28.94	36.7	71.06	63.2
LP(1) N3	1.9395	1.9261					$sp^{2.45}$	$sp^{2.31}$	28.99	30.24	71.01	69.76
LP(1)O11	1.9847	1.9120					$sp^{1.12}$	$sp^{2.31}$	47.2	30.18	52.8	69.82

BD−2-centred bonding; ED−electron density; ED_A −electron density of 'A' atom; ED_B electron density of 'B' atom; LP −lone pair

Table 9: The second order perturbation energies $E^{(2)}$ (kcal/mol)corresponding to the most important charge transfer interactions (donor-acceptor) in the compound studied by HF/6-311G and B3LYP/ 6-311G method.

Donor NBO (i)	Acceptor NBO (j)	HF			B3LYP		
		$E^{(2)}$ kcal/mol	E(j)-E (i) a.u	F(i,j) a.u	$E^{(2)}$ kcal/mol	E(j) − E (i) a.u	F(i,j) a.u
BD (1) N 1 - C 6	BD*(1) C 2 - C 7	3.25	1.64	0.065	2.34	1.59	0.054
BD (1) N 1 - C 6	BD*(1) C 5 - C 6	1.68	1.85	0.05	1.1	1.76	0.039
BD (1) N 1 - C 6	BD*(1) C 5 - H 13	2.25	1.72	0.056	0.61	1.83	0.030
BD (1) C 2 - N 3	BD*(1) C 2 - C 7	0.74	1.66	0.031	0.57	1.16	0.023
BD (1) C 2 - C 7	BD*(1) N 1 - C 2	1	1.52	0.035	3.4	1.05	0.054
BD (1) C 2 - C 7	BD*(1) N 1 - C 6	4.67	1.53	0.075	1.18	1.41	0.037
BD (1) C 2 - C 7	BD*(1) C 2 - N 3	0.95	1.52	0.034	1.13	1.41	0.036
BD (1) C 2 - C 7	BD*(1) N 3 - C 4	4.8	1.51	0.076	0.76	1.05	0.025
BD (1) C 2 - C 7	BD*(1) C 7 - H 8	0.62	1.48	0.027	3.77	1.06	0.057
BD (1) C 4 - C 5	BD*(1) C 5 - C 6	4.28	1.78	0.078	0.61	1.86	0.03
BD (1) C 4 - C 5	BD*(1) C 5 - H 13	2.22	1.65	0.054	0.52	1.16	0.022

BD (1) C 5 - C 6	BD*(1) N 1 - C 6	1.33	1.65	0.042	1.33	1.15	0.035
BD (1) C 5 - C 6	BD*(1) C 4 - C 5	4.34	1.74	0.078	0.61	1.92	0.031
LP (1) N 1	BD*(1) C 2 - N 3	13.17	1.19	0.113	2.16	1.74	0.055
LP (1) N 1	BD*(1) C 2 - C 7	1.76	1.11	0.04	2.82	1.12	0.051
LP (1) N 1	BD*(1) C 5 - C 6	10.77	1.32	0.107	0.81	1.28	0.029
LP (1) N 3	BD*(1) N 1 - C 2	12.19	1.21	0.109	3.03	1.16	0.054
LP (1) N 3	BD*(1) C 2 - C 7	1.68	1.12	0.039	3.02	1.13	0.053
LP (1) N 3	BD*(1) C 4 - C 5	9.86	1.3	0.102	0.67	1.3	0.027
LP (1) O 11	BD*(1) N 3 - C 4	7.51	1.53	0.096	2.94	1.36	0.058

BD−2-centred bonding; LP –lone pair; BD*− 2-centred anti-bonding
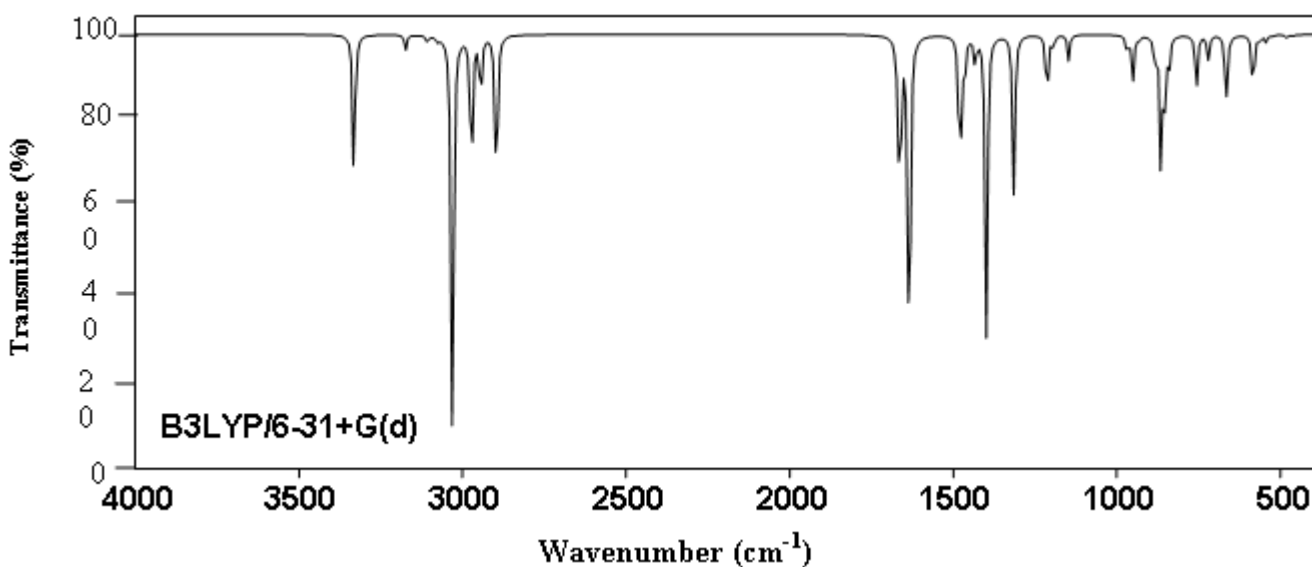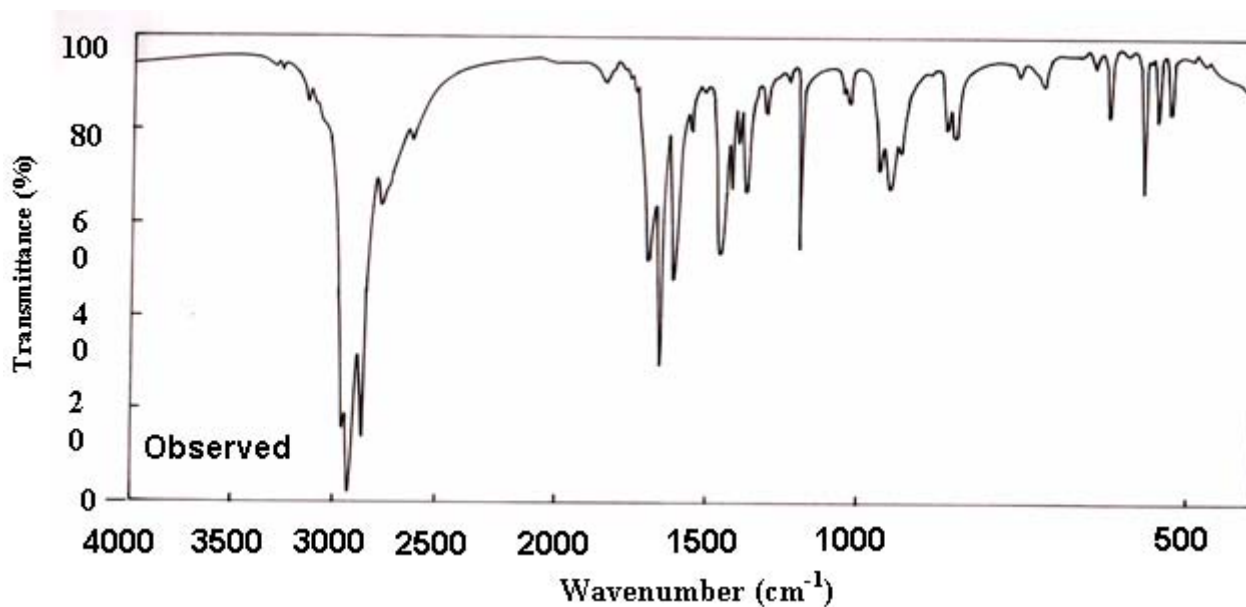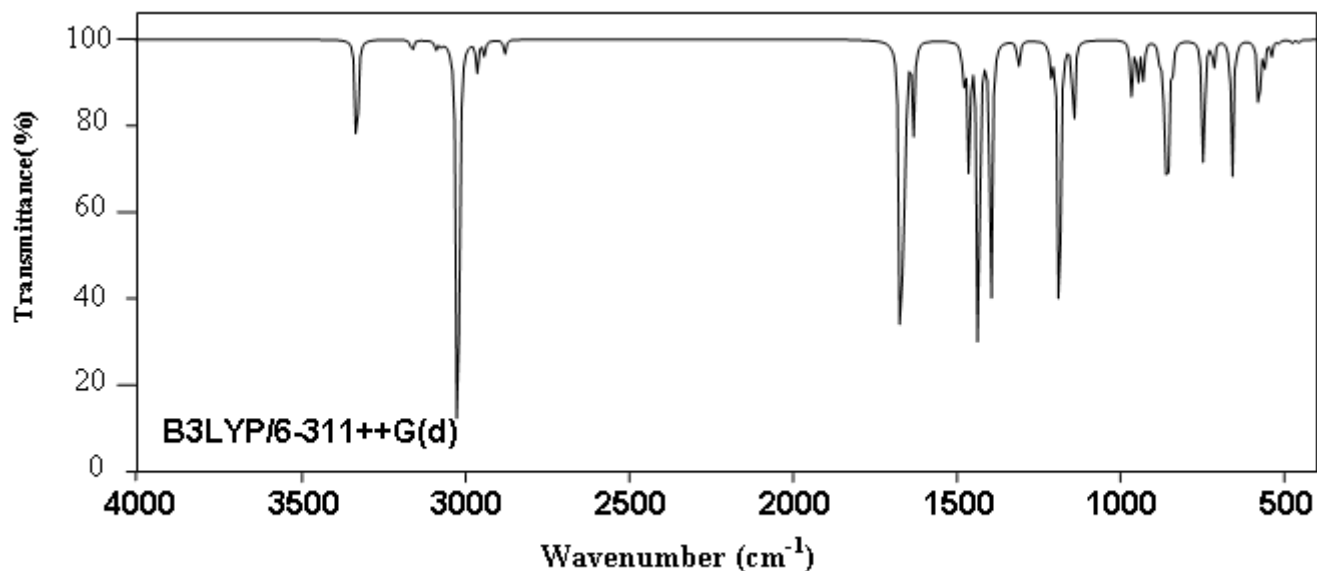
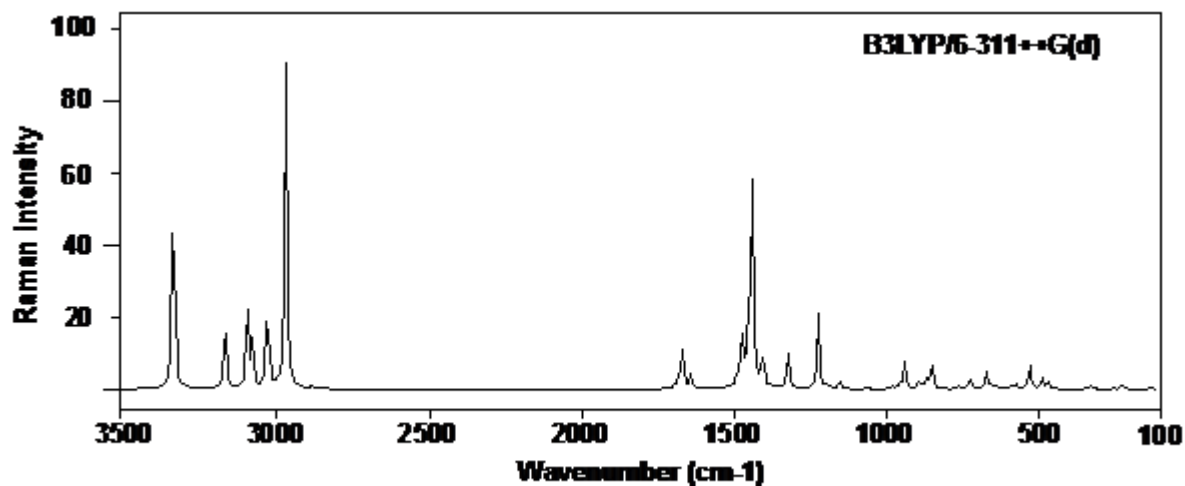Fig. 8.1 Observed and calculated infrared spectra of 4-hydroxy-2,6-dimethylpyrimidine

Paper ID: ART20163751
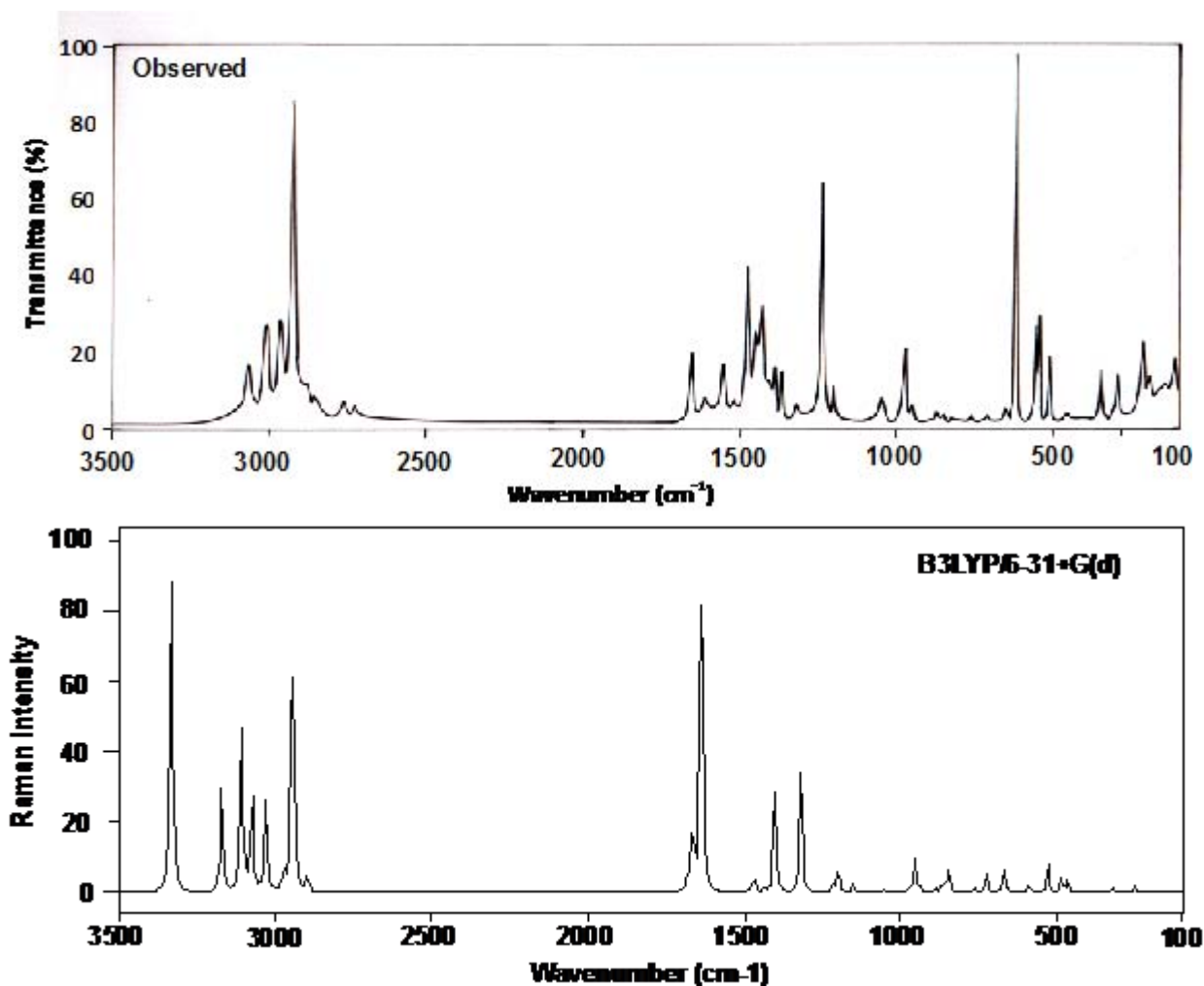
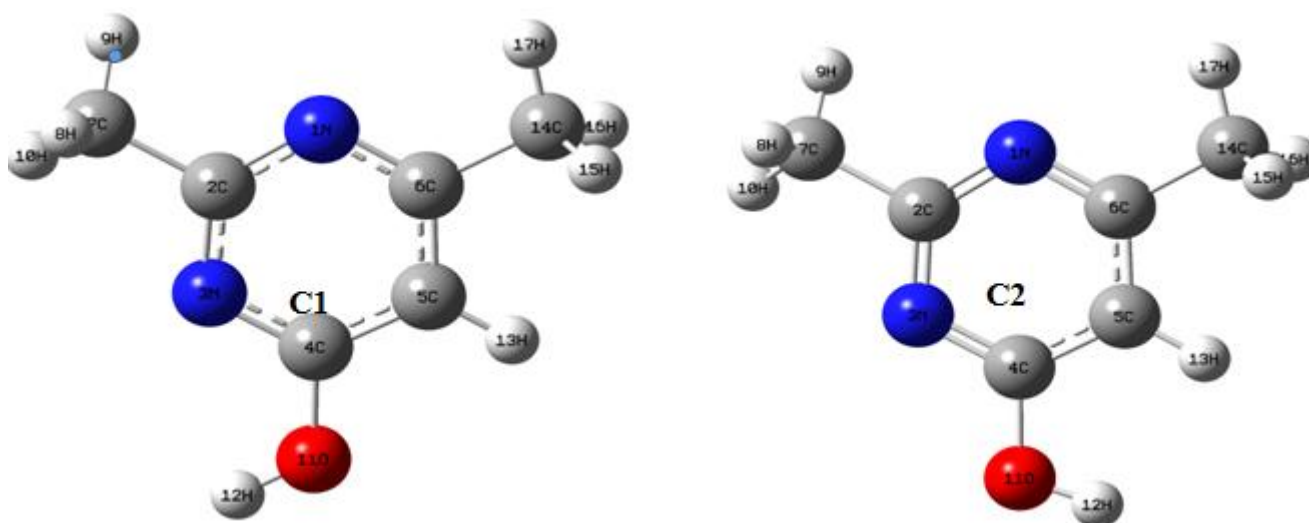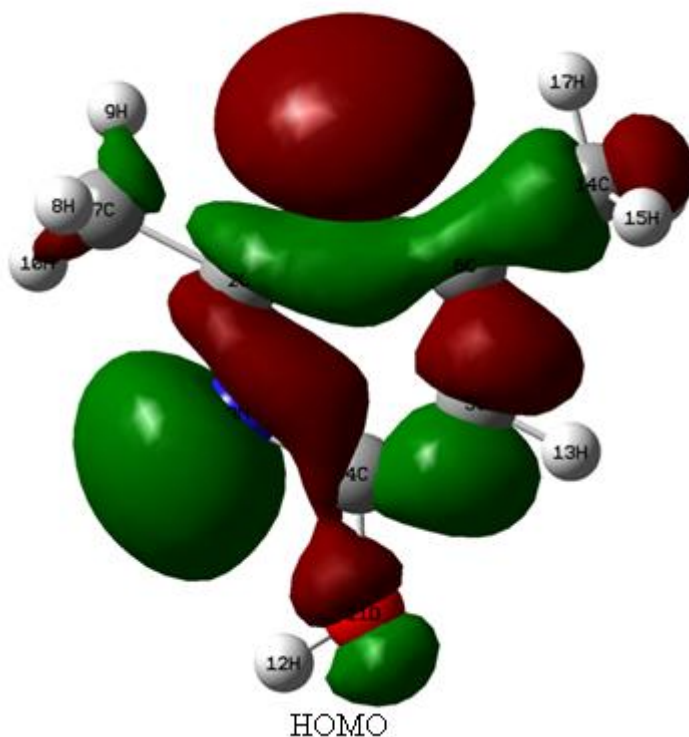Fig. 8.2 Observed and calculated Raman spectra of 4-hydroxy-2,6-dimethylpyrimidine

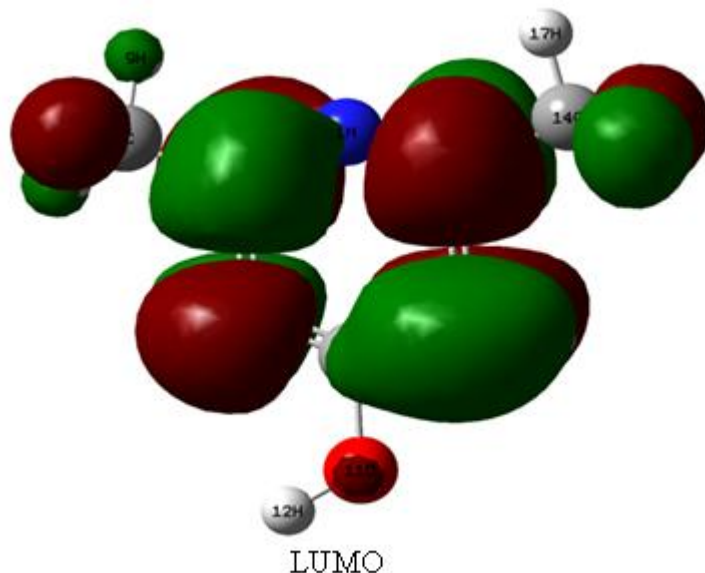**Figure 3:** Possible conformers of 4-hydroxy-2,6-dimethylpyrimidine

HOMO

Paper ID: ART20163751

LUMO

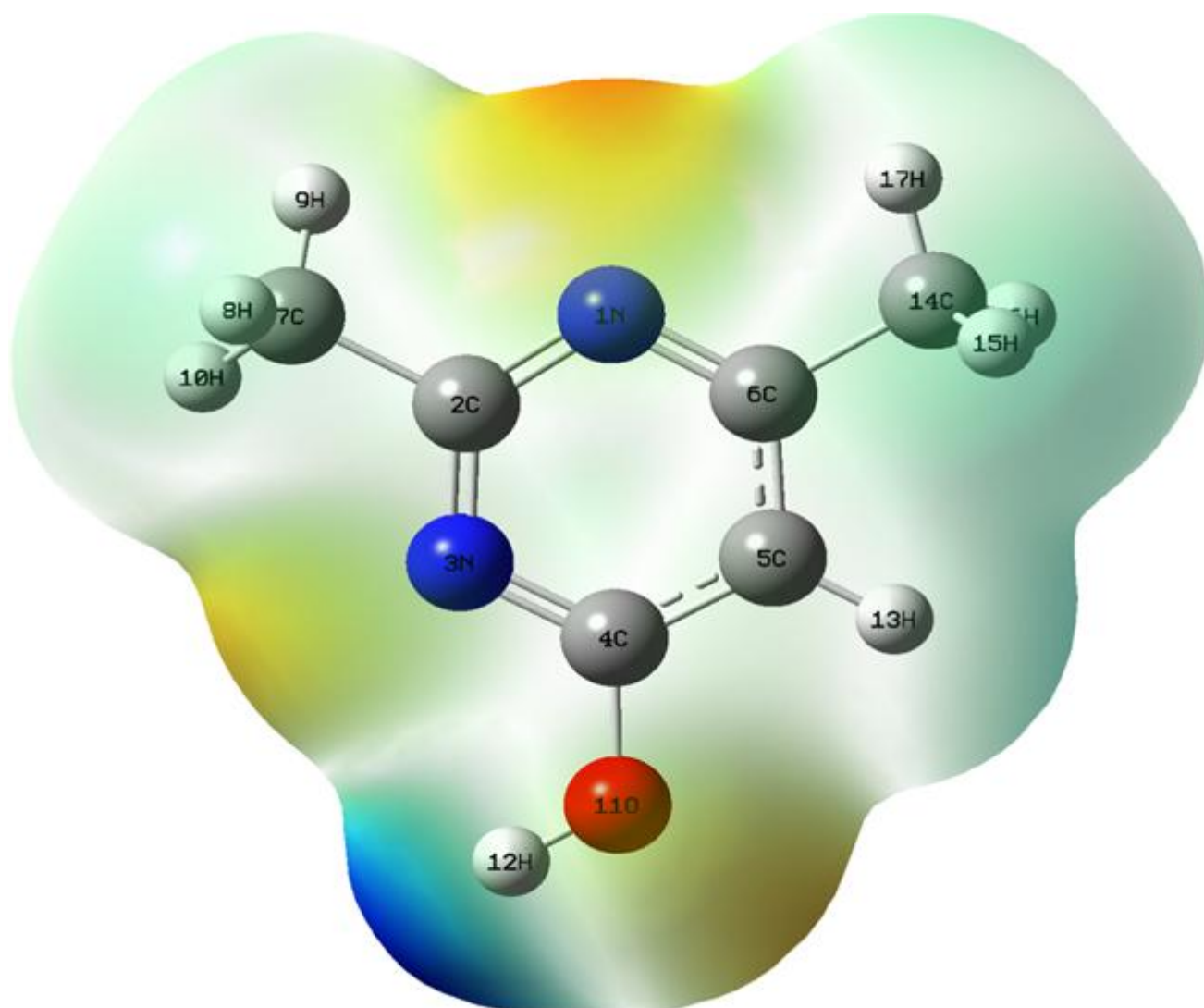**Fig. 4** The 3D plots of the HOMO and LUMO surface of the HDMP

Figure 5: Electrostatic potential surface of the HDMP